Topological phases of nonsymmorphic crystals: Shastry-Sutherland lattice at integer filling

Hyeok-Jun Yang* and SungBin Lee†
Department of Physics, Korea Advanced Institute of Science and Technology, Daejeon 34141, Korea

(Received 10 October 2018; published 25 April 2019)

Motivated by intertwined crystal symmetries and topological phases, we study the possible realization of topological insulators in nonsymmorphic crystals at integer fillings. In particular, we consider spin-orbit-coupled electronic systems of two-dimensional crystal Shastry-Sutherland lattices at integer filling where the gapless line degeneracy is protected by glide reflection symmetry. Based on a simple tight-binding model, we investigate how the topological insulating phase is stabilized by breaking nonsymmorphic symmetries but in the presence of time reversal symmetry and inversion symmetry. In addition, we also discuss the regime where Dirac semimetal is stabilized, having nontrivial Z_2 invariants even without spin-orbit coupling. Our study can be extended to more general cases where all lattice symmetries are broken and we also discuss possible application to topological Kondo insulators in nonsymmorphic crystals where crystal symmetries can be spontaneously broken as a function of the Kondo coupling.

DOI: 10.1103/PhysRevB.99.165140

I. INTRODUCTION

In the thermodynamic limit, the gapped or gapless nature of phases is an important characteristic for classification of low-energy excitations and their physical properties. For noninteracting systems, one can predict a so-called band insulator where the filling is an integer, i.e., the unit cell must contain an integer number of electrons per unit cell and spin, thus the band can be completely filled below the Fermi energy [1]. On the other hand, the Mott insulator is a counter example of a band insulator where the insulating phase with all symmetries conserved is realized even at fractional filling [2,3]. For this case, the celebrated Hastings-Oshikawa-Lieb-Schultz-Mattis (HOLSM) theorem gives strong guiding principles for any fractional filling no matter what types of particles and interaction strengths are used; if the system at fractional filling does preserve all the symmetries, it must be either gapless or gapped with degenerate ground states that accompany fractional low-energy excitations [4–8].

In crystals, it turns out that discrete lattice symmetries can give similar constraints even at integer fillings [9–13]. In particular, it holds for nonsymmorphic crystals whose space-group symmetries are not represented by a direct product of translation and point group symmetry, thus they always contain glide reflections or screw rotations. These symmetries accompany fractional (say $1/\mathcal{S}$) translation followed by either reflection or rotational symmetries. Attributed to such fractional translation, the filling ν to be a trivial insulator is typically a multiple of the specific integer $\mathcal{S}$, i.e., $\nu = n\mathcal{S}$, $n \in Z$. Here, we emphasize that the filling ν is defined as the average number of electrons in a unit cell for each spin polarization. For any other integer fillings ($\nu \notin n\mathcal{S}$), one can still apply HOLSM theorem and the system with preservation of all the symmetries must be categorized into two cases: (i) gapless and (ii) gapped with fractional low-energy excitations [14]. This strong argument indicates that if we ignore the exotic scenario of Mott insulating phases with fractional low-energy excitations, then the gaplessness of the system is protected by nonsymmorphic crystal symmetries at certain integer fillings $\nu \notin n\mathcal{S}$ [15–18].

One intriguing question is then how the system drives into the transition from gapless semimetal to gapped insulating phase by breaking nonsymmorphic crystal symmetries. In particular, when the electronic system is described by heavy ions, the spin-orbit coupling (SOC) effect plays an important role and it is natural to consider the interplay of nonsymmorphic symmetry breaking and SOC results in unique topological insulating phases [19,20]. Such a gapped phase can be generally favored to reduce the kinetic energy of electrons, thus it gives rise to instability of the gapless semimetallic phase protected by either glide reflection symmetry or screw rotation symmetry at integer filling. Therefore, it can drive the system into an insulating phase with spontaneous breaking of nonsymmorphic crystal symmetries, accompanied by lattice distortion and formation of charge (spin) ordering [21]. Furthermore, one can also expect our scenario to be applicable to the Kondo lattice system in nonsymmorphic crystals [22,23]. When localized magnetic moments and itinerant electrons are both present, control of the Kondo coupling strength can derive multiple phase transitions. At particular integer fillings of itinerant electrons, an intermediate Kondo coupling leads to partial Kondo screening in such a way that all lattice symmetries are broken. Then the system can be driven into a *topological Kondo insulator* with spontaneously broken nonsymmorphicity, which is a natural extension of work done in Ref. [24].

In this paper, we investigate the possible phase transition from a gapless semimetal protected by nonsymmorphic crystal symmetry to a topological insulator where the crystal symmetries are broken but edge states are protected by

*yang267814@kaist.ac.kr
†sungbin@kaist.ac.kr

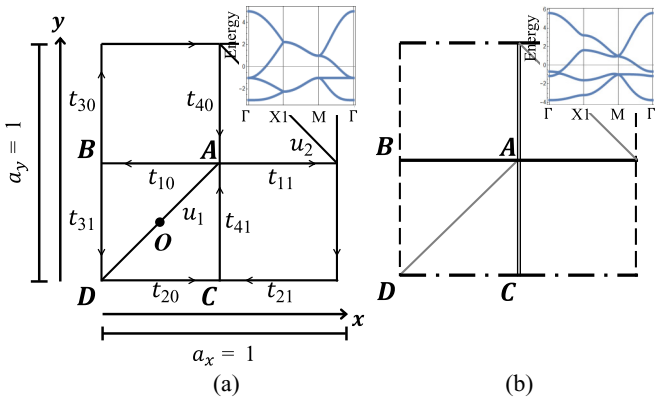

FIG. 1. (a) Shastry-Sutherland lattice with nearest-neighbor hopping parameters t_{ij} and u_i. The arrow on each link indicates the direction of symmetry-allowed SOC. Inset: Bulk dispersion when all parameters are equal to 1. Along the line X1-M, the first and second bands (third and fourth bands) are degenerate and these degeneracies are protected by glide reflection symmetry. (b) In the Shastry-Sutherland lattice, solid, dashed, dash-dotted, and double lines indicate distinct electron hopping configurations which break all lattice symmetries. Inset: Bulk dispersion with all distinct hoppings represented by different line styles. The line degeneracy along X1-M is absent but the degeneracy at point M is still present.

time-reversal symmetry [25–27]. We exemplify our scenario by a spin-orbit-coupled electronic system in a specific two-dimensional crystal, the Shastry-Sutherland lattice (SSL) [28]. Especially, we focus on the filling $\nu = 1$ per unit cell and spin where the gapless electronic structure at the Fermi level is protected by glide reflection symmetry. Considering two ways of breaking the glide reflection symmetry, the stabilities of the trivial insulator and topological insulator are addressed as functions of the electron hopping and strength of SOC [15,29]. Based on the calculation of Z_2 invariants [30,31], we show a large parameter space where the topological insulating phase is indeed stabilized. Furthermore, we discuss the parameter space where an odd number of gapless Dirac points must be present in the absence of SOC. We note that a similar argument can be easily extended to other nonsymmorphic crystals including both two-dimensional and three-dimensional lattices.

II. BAND PROPERTIES IN NONSYMMORPHIC SSL

Focusing on the electronic band structure of nonsymmorphic crystals, we explore how nosymmorphic symmetry breaking leads to nontrivial topological insulating phases. In particular, we employ the simple tight-binding model on the SSL (space group $p4g$) with nearest-neighbor hoppings including the horizontal ($-$), vertical ($|$), and diagonal ($/$) directions,

$$H_0 = \sum_{\sigma,\langle i,j\rangle\in|,-} t_{ij} c^\dagger_{i\sigma} c_{j\sigma} + \sum_{\sigma,\langle i,j\rangle\in/} u_{ij} c^\dagger_{i\sigma} c_{j\sigma}, \qquad (1)$$

where $c^{(\dagger)}_{i,\sigma}$ indicates the (creation) annihilation operator at site i and spin σ. Each hopping parameter t_{ij} and u_{ij} is depicted in Fig. 1(a). For simplicity, all t_{ij} and u_{ij} are chosen to be positive and spin independent. Henceforth, we particularly focus on the filling $\nu = 1$ per unit cell and spin, but without losing generality a similar argument can be made for another case, $\nu = 3$.

First, let us consider the spinless system with each unit cell containing one electron on average, thus filling $\nu = 1$. The unit cell of the SSL contains four sites and lattice symmetries such as inversion P, C_4 rotation, and mirror symmetries $M_{\hat{x}+\hat{y}}$ and $M_{-\hat{x}+\hat{y}}$ are present when the hopping parameters t_{ij} are all the same and $u_1 = u_2$ [see Fig. 1(a)] [28,32]. In addition, the glide reflection symmetries G_x and G_y defined by half-translations along the x, y direction, followed by the mirror reflections $M_{\hat{y}}$ and $M_{\hat{x}}$, are present. The inset in Fig. 1(a) shows a band structure along the lines with high symmetry points $\Gamma(0,0)$, $\mathrm{X1}(\pi,0)$ [$\mathrm{X2}(0,\pi)$], and $\mathrm{M}(\pi,\pi)$. At $\nu = 2$, the system is gapless at Γ and becomes a semimetal [33]. For $\nu = 1$ and 3, one can see that the first and second bands (third and fourth bands) are degenerate along lines X1-M and X2-M. These line degeneracies are protected by glide reflection symmetries G_x and G_y, respectively. In the absence of spins, $G_x^2 = e^{ik_x} = -1$ along the Brillouin zone boundary $k_x = \pi$. Then there exists additional degeneracy related by $[h_0(\pi, k_y), G_x\Theta] = 0$ and $(G_x\Theta)^2 = -1$, where $h_0(k_x, k_y)$ is the Hamiltonian matrix for Eq. (1) at momentum (k_x, k_y) and $\Theta = K$ is the complex-conjugate operator. Similarly, the invariant line $k_y = \pi$ has a line degeneracy protected by $G_y\Theta$. Our argument is carried out within band theory, however, the validity of line degeneracy holds in the presence of interactions as long as the symmetry is preserved [15,34].

The insulating phases at $\nu = 1$ and 3 thus always require breaking of G_x and G_y symmetries, but interestingly, within the simple tight-binding model, the inverse is not always true. Suppose a system in which electrons with s orbitals sit on an SSL at integer filling. The spin degrees of freedom is not considered yet. The Hamiltonian in momentum space can be rewritten as $H_0 = \Sigma_{\mathbf{k}} \psi^\dagger_{\mathbf{k}} h_0(\mathbf{k}) \psi_{\mathbf{k}}$, where $\psi_{\mathbf{k}} = (c_{\mathbf{k},A}, c_{\mathbf{k},B}, c_{\mathbf{k},C}, c_{\mathbf{k},D})^T$ and $c^{(\dagger)}_{\mathbf{k},\alpha}$ is the annihilation (creation) operator at momentum $\mathbf{k}$ on sublattice α. When the t_{ij} values are all equivalent and $u_1 = u_2$, the Hamiltonian at point M can be readily analyzed. The eigenspace at point M is spanned by $|\Psi 1_\pm\rangle = \frac{1}{\sqrt{2}}(c^\dagger_{M,A} \pm c^\dagger_{M,D})|0\rangle$ and $|\Psi 2_\pm\rangle = \frac{1}{\sqrt{2}}(c^\dagger_{M,B} \pm c^\dagger_{M,C})|0\rangle$, with eigenvalues $\pm u_1$ for occupied ($-$) and unoccupied ($+$) eigenspaces, respectively. In order to open a gap, these states need to be coupled through the Hamiltonian, e.g., $\langle \Psi 2_a | h_0(M) | \Psi 1_a \rangle \neq 0$. One may think that breaking the lattice symmetries by varying the hopping parameters t_{ij} and u_i leads to finite couplings between $|\Psi 1_a\rangle$ and $|\Psi 2_a\rangle$ and, thus, to opening a gap in the system. However, there exists the case where, with breaking of all lattice symmetries, their coupling is still 0. In Fig. 1(b), the links sketched in the same style indicate the identical hopping parameters along the links, i.e., $t_{10} = t_{11}$, $t_{20} = t_{21}$, $t_{30} = t_{31}$, $t_{40} = t_{41}$. This configuration breaks all lattice symmetries but the degeneracy at point M is preserved. [See the band structure in the inset in Fig. 1(b).] The reason is as follows. In $\mathbf{k}$ space, the electron hoppings between sublattices are performed by consuming a phase of the wave packet. At point M, the phases from one site to another on sublattices along the x, y directions are cooperatively canceled, thus their off-diagonal components of $h_0(M)$ vanish, resulting in degenerate bands at point M. Of

course, the different hopping parameters between the $\hat{x}/2$ and the $-\hat{x}/2$ directions (similarly for the $\hat{y}$ direction) will lead the system to be gapped; this is discussed below.

Now let us consider the spinful electronic system. Including spin degeneracy, there exist eight bands in total and each two bands are degenerate since Kramers doublet $(P\Theta)^2 = -1$. Thus, at fillings $\nu = 1$ and $\nu = 3$ (per unit cell and spin), four bands are degenerate along X1-M and X2-M as shown in Fig. 1(a) (two from Kramers doublet and two from glide reflection symmetries). The intrinsic SOC can be included as an imaginary hopping term,

$$H_{\mathrm{SO}} = \sum_{\langle i,j\rangle,\sigma} i\sigma_z d_{ij} c^{\dagger}_{i\sigma} c_{j\sigma}, \tag{2}$$

where $d_{ij} = \pm\lambda$ indicates the SOC strength, having relative signs depicted in Fig. 1(a). (The arrow toward i from j defines $d_{ij} = +\lambda$.) In the presence of intrinsic SOC, the total spin S_z is still conserved so one can consider the system for each spin independently. For each spin sector, this imaginary hopping can be considered as an effective magnetic flux resulting in nontrivial insulating phases [29,35,36]. This SOC term opens a gap at half-filling $\nu = 2$ and leads to a topological insulating phase, in the same manner as discussed in graphene at half-filling [29,36]. In this case, the filling is a multiple integer of the fractional translation $\mathcal{S} = 2$, thus the HOLSM theorem is silent and the system can be either gapless or gapped depending on the controlling parameters [9,37]. Indeed, the presence or absence of SOC makes the system either gapless or gapped at this filling.

III. BROKEN GLIDE REFLECTION SYMMETRIES AND TOPOLOGICAL PHASES

At fillings $\nu = 1$ and 3, the band degeneracies along X1-M and X2-M are protected by glide reflection symmetry [15]. To explore how band degeneracies split and the system goes into an insulating phase, we can consider two particular cases that break glide reflection symmetries illustrated in Fig. 2:

$$\begin{aligned}
&\text{(i) Fig. 2(a):} \quad \tilde{t}_1 \equiv t_{10} = t_{20} = t_{31} = t_{41},\\
&\qquad\qquad\quad\ \ \tilde{t}_2 \equiv t_{11} = t_{21} = t_{30} = t_{40}.\\
&\text{(ii) Fig. 2(b):} \quad \tilde{t}_3 \equiv t_{10} = t_{20} = t_{30} = t_{40},\\
&\qquad\qquad\quad\ \ \tilde{t}_4 \equiv t_{11} = t_{21} = t_{31} = t_{41}, \quad \tilde{u} \equiv u_1 = u_2.
\end{aligned} \tag{3}$$

For Eq. (3), case (i), the system preserves two mirror reflections $M_{\hat{x}\pm\hat{y}}$ but breaks all other symmetries, G_x, G_y, and C_4, whereas in case (ii), the system preserves C_4 but breaks G_x, G_y, and $M_{\hat{x}\pm\hat{y}}$. In both cases, glide symmetries are broken. The SOC strength d_{ij} is also modified based on the broken spatial symmetries in each case, (i) and (ii). As depicted in Figs. 2(a) and 2(b), the deviation of SOC is represented as the ratio of two adjacent strengths δ. When $\delta = 1$, the SOC term recovers the full lattice symmetries of the original Shastry-Sutherland lattice.

For given parameters, we evaluate the topological invariant, which is the product of the parities of the occupied eigenstates at four different time-reversal-invariant momentum (TRIM) points in the Brillouin zone [30]. In two dimensions, the negative sign indicates a topological phase and the positive sign indicates a trivial phase. In both cases in Eq. (3) (see also Fig. 2), the products of parities at X1 and X2 are related to each other. For case (i) in Eq. (3), it satisfies $M^{\dagger}_{\pm\hat{x}+\hat{y}} P M_{\pm\hat{x}+\hat{y}} = P$, thus the parities at X1 and X2 are the same. For case (ii), however, $C_4^{\dagger} P C_4 = e^{-i(k_x+k_y)} P = -P$ and the parities at X1 and X2 are opposite. Thus, one only needs to examine whether or not the parities at points Γ and M are the same. As a result, the system at filling $\nu = 1$ becomes a topological phase under the conditions

$$\begin{aligned}
&\text{(i)} \quad \sqrt{\tilde{t}_-^2 + u_-^2} - \sqrt{\tilde{\lambda}_-^2 + u_-^2} < 2u_+ < \sqrt{\tilde{t}_+^2 + u_-^2} - \sqrt{\tilde{\lambda}_+^2 + u_-^2},\\
&\text{(ii)} \quad \tilde{u} > \tilde{t}_3 + \tilde{t}_4 - |\tilde{\lambda}_+/4| \ \text{ and } \ \tilde{u} > -|\tilde{t}_3 - \tilde{t}_4| + |\tilde{\lambda}_-/4|,
\end{aligned} \tag{4}$$

where $\tilde{t}_\pm = 4(\tilde{t}_1 \pm \tilde{t}_2)$, $u_\pm = u_1 \pm u_2$, and $\tilde{\lambda}_\pm = 4\lambda(1 \pm \delta)$. The conditions are also satisfied when the signs of inequality are all reversed in Eq. (4).

Based on the conditions in Eq. (4), possible parameter space for topological and trivial phases is shown in Fig. 3. Figures 3(a) and 3(b) show the phase diagrams for case (i) [see also Fig. 2(a)] as functions of $\lambda/\tilde{t}_1$ and $\tilde{t}_2/\tilde{t}_1$ with $u_1 = 2$, $u_2 = 4$; there are two parameter sets, for $\delta = -2$ [Fig. 3(a)] and for $\delta = 2$ [Fig. 3(b)]. Figures 3(c) and 3(d) represent the phase diagrams for case (ii) [see also Fig. 2(b)] as functions of $\lambda/\tilde{t}_3$ and $\tilde{t}_4/\tilde{t}_3$ with $u_1 = u_2 = 1$, for $\delta = -2$ [Fig. 3(c)] and for $\delta = 2$ [Fig. 3(d)]. In Figs. 3(a)–3(d), blue and white regions indicate where topological insulating phases and trivial insulating phases are stabilized if the system is gapped. At the phase boundaries separating the two distinct phases, the gap should be closed at least one momentum point to exchange the parities with the unoccupied bands. As shown in Fig. 3, there exists a large parameter regime for small SOC where topological insulating phases are stabilized with glide reflection symmetry breaking.

Figure 4 shows the one-dimensional band structure in a strip geometry for three distinct cases [29,38–41]. Figures 4(a)

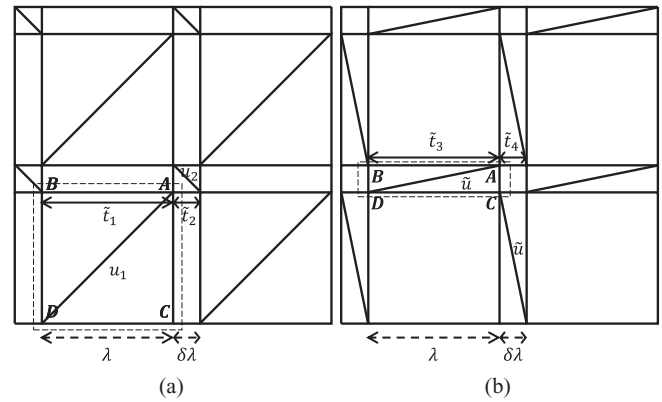

FIG. 2. Distorted Shastry-Sutherland lattice with broken glide reflection symmetries but preservation of mirror or rotation symmetries: (a) preservation of mirror symmetries with hopping parameters defined as in Eq. (3), case (i); (b) preservation of C_4 rotation symmetry with hopping parameters defined as in Eq. (3), case (ii). Dashed boxes indicate the unit cell, which includes four sublattices: A, B, C, and D. δ measures the relative distortion in SOC. By parametrizing $\tilde{t}_i$, λ, and δ, Fig. 3 shows the region where topological insulating phases are stabilized. See the text for more details.

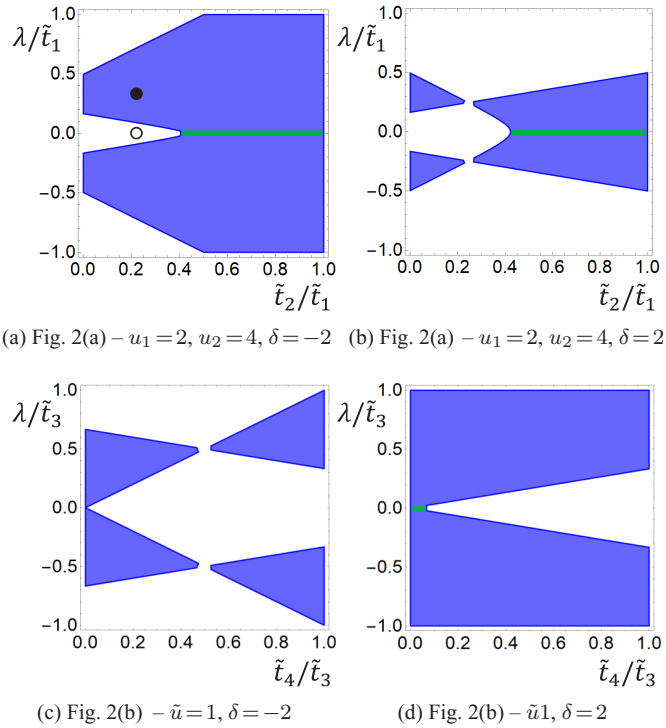

(a) Fig. 2(a) – $u_1 = 2$, $u_2 = 4$, $\delta = -2$ (b) Fig. 2(a) – $u_1 = 2$, $u_2 = 4$, $\delta = 2$

(c) Fig. 2(b) – $\tilde{u} = 1$, $\delta = -2$ (d) Fig. 2(b) – $\tilde{u}1$, $\delta = 2$

FIG. 3. Phase diagrams of trivial and topological insulators for gapped systems, as functions of $\tilde{t}_2/\tilde{t}_1$ and $\lambda/\tilde{t}_{1(3)}$: (a, b) for the distorted lattice structure illustrated in Fig. 2(a); (c, d) for the cases illustrated in Fig. 2(b). Blue and white regions represent where the topological insulator and trivial insulator are stabilized, respectively. In the green region at $\lambda = 0$ is the Z_2 invariant is -1 and Dirac points or Fermi arcs enclosing Dirac points are stabilized.

and 4(b) show the edge spectra at parameters represented by open and filled circles in Fig. 3(a), respectively. One can easily see the absence or presence of edge modes for the trivial insulator or topological insulator. Figure 4(c) is the edge spectrum for a topological insulator with parameters deviating from the case for Fig. 4(b), in such a way that the system additionally breaks the inversion symmetry. More explicitly, we keep all the same parameters except $\tilde{t}_2$ defined in Eq. (3) but take $t_{11} = t_{40} = 1.3$, $t_{21} = 2.5$, and $t_{30} = 3$

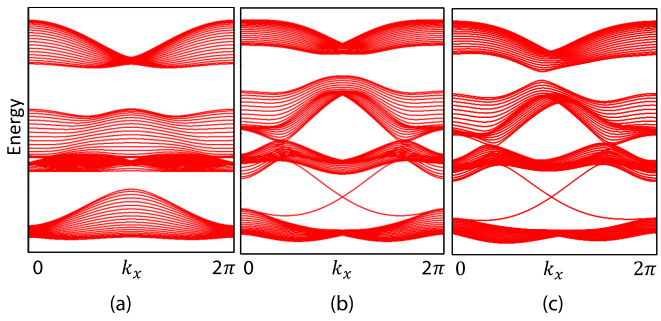

FIG. 4. Edge spectra for trivial and topological insulating phases. (a) Trivial insulator with parameters at the open circle shown in Fig. 3(a). (b) Topological insulator with parameters at the filled circle shown in Fig. 3(a). (c) Topological phase with parameters which additionally break inversion symmetry from (b). See the text for more details.

to break the inversion symmetry. It is noteworthy that this topological phase is protected by time-reversal symmetry, not by inversion symmetry. These edge states are stable under any small perturbation as long as the perturbation respects time-reversal symmetry. Although the simple analysis of the Z_2 invariant at TRIM points no longer works, the topological phase survives even when the inversion symmetry is explicitly broken as shown in Fig. 4(c).

Our analysis so far can be extended beyond the nearest-neighbor tight-binding model and one can still use the indicator Eq. (4) to explore the parameter regime where the topological insulator is stabilized. We note that several types of long-range electron hoppings simply enhance the nearest-neighbor hopping parameters in each case discussed for Eq. (4). In order to see this, let us consider the long-range electron hopping between sublattice α and sublattice β with magnitude δt across the relative distance (m, n) in units of the unit cell (a_x, a_y). Then the Hamiltonian matrix component in momentum space has the additional term $\delta t e^{i(k_x m + k_y n)}$. In both case (i) and case (ii) in Eq. (3) (see Fig. 2), any long-range hopping connecting sublattices A and B and their symmetry-related hopping results in $\tilde{t}_{1,3} \to \tilde{t}_{1,3} + \delta$ if $m + n$ is even and $\tilde{t}_{2,4} \to \tilde{t}_{2,4} + \delta$ if $m + n$ is odd. Here, evenness and oddness have nothing to do with symmetries but are related to the choice of unit cell shown in Fig. 2. A similar analysis can be also done for other parameters, u_1, u_2, and $\tilde{u}$.

We address another important aspect in our analysis. Through the entire derivation, we have assumed that if the system is gapped, the topological phases are stabilized with a given parameter regime as shown in Eq. (4) and Fig. 3. However, analyzing the Z_2 invariants at the TRIM points does not always guarantee an insulating phase. Rather, if the system is an insulating phase, it diagnoses whether the trivial insulator or topological insulator is stabilized. Thus, there may be accidental gapless points away from the TRIM points in the Brillouin zone. Therefore, it is possible to obtain a negative sign of Z_2 invariants even in the absence of SOC and this originates from the odd number of Dirac cones which are not necessarily at the TRIM points and lead to π Berry phases [30,33]. As shown in Fig. 3, there exists a wide range of parameter space, represented by the horizontal green line, where the Z_2 invariant is negative in the absence of SOC. In this regime, the system must contain an odd number of Dirac cones. For case (i) in Eq. (3), mirror symmetries guarantee an odd number of gapless Dirac points to be along the line between Γ and M. In case (ii) in Eq. (3), the fourfold rotational symmetry enforces that the gapless point is located at point Γ or M, and this indeed happens at $\nu = 1$ and $\nu = 3$ with the given parameter set (horizontal green line) in Fig. 3(d).

IV. CONCLUSIONS

Based on our studies, one may expect that nonsymmorphic symmetry breaking could give rise to the phase transition from gapless metal to gapped trivial or topological insulating phases. Hence, a system with strong coupling between lattice and electronic degrees of freedom may favor spontaneous lattice distortion. Due to the additional energy gain upon opening the gap, the system may form charge or spin order in such a way that the system breaks nonsymmorphic

symmetries. Relevant future work would be to explore this using the first-principle calculation. In addition, one can also imagine a possible topological Kondo insulator in nonsymmorphic crystals. In particular, the Kondo lattice model in nonsymmorphic crystals can show interesting behavior in the intermediate Kondo coupling [24]. In this case, the system spontaneously breaks nonsymmorphic symmetry and opens a gap where a Kondo insulator is energetically favored. Therefore, depending on how the system breaks nonsymmorphicity, the system can spontaneously drive the phase transition from Kondo semimetal to topological Kondo insulator as a function of the Kondo coupling strength. Our results provide insight into the important role of lattice symmetries and their relevance to topological phase transitions and pave the way for exploration of relevant materials and experiments in future.

ACKNOWLEDGMENTS

We would like to thank S. Parameswaran for useful discussions and comments. H.-J.Y. and S.B.L. were supported by the KAIST startup and National Research Foundation Grant No. NRF-2017R1A2B4008097.

[1] P. Fazekas, *Lecture Notes on Electron Correlation and Magnetism* (World Scientific, Singapore, 1999), Vol. 5.
[2] N. F. Mott and L. Friedman, Philos. Mag. **30**, 389 (1974).
[3] N. Mott, *Metal-Insulator Transitions* (CRC Press, Boca Raton, FL, 1990).
[4] E. Lieb, T. Schultz, and D. Mattis, Ann. Phys. **16**, 407 (1961).
[5] M. Oshikawa, Phys. Rev. Lett. **84**, 1535 (2000).
[6] M. B. Hastings, Phys. Rev. B **69**, 104431 (2004).
[7] M. Hastings, Europhys. Lett. **70**, 824 (2005).
[8] A. M. Essin and M. Hermele, Phys. Rev. B **90**, 121102(R) (2014).
[9] S. A. Parameswaran, A. M. Turner, D. P. Arovas, and A. Vishwanath, Nat. Phys. **9**, 299 (2013).
[10] A. König and N. D. Mermin, Phys. Rev. B **56**, 13607 (1997).
[11] A. König and N. D. Mermin, Am. J. Phys. **68**, 525 (2000).
[12] H. Watanabe, H. C. Po, A. Vishwanath, and M. Zaletel, Proc. Natl. Acad. Sci. U.S.A. **112**, 14551 (2015).
[13] H. Watanabe, H. C. Po, M. P. Zaletel, and A. Vishwanath, Phys. Rev. Lett. **117**, 096404 (2016).
[14] S. B. Lee, M. Hermele, and S. A. Parameswaran, Phys. Rev. B **94**, 125122 (2016).
[15] S. M. Young and C. L. Kane, Phys. Rev. Lett. **115**, 126803 (2015).
[16] L. Michel and J. Zak, Phys. Rev. B **59**, 5998 (1999).
[17] A. Topp, J. M. Lippmann, A. Varykhalov, V. Duppel, B. V. Lotsch, C. R. Ast, and L. M. Schoop, New J. Phys. **18**, 125014 (2016).
[18] S. A. Ekahana, S.-C. Wu, J. Jiang, K. Okawa, D. Prabhakaran, C.-C. Hwang, S.-K. Mo, T. Sasagawa, C. Felser, B. Yan *et al.*, New J. Phys. **19**, 065007 (2017).
[19] J. Cano, B. Bradlyn, Z. Wang, L. Elcoro, M. G. Vergniory, C. Felser, M. I. Aroyo, and B. A. Bernevig, Phys. Rev. Lett. **120**, 266401 (2018).
[20] J. Sinova, D. Culcer, Q. Niu, N. A. Sinitsyn, T. Jungwirth, and A. H. MacDonald, Phys. Rev. Lett. **92**, 126603 (2004).
[21] P. Coleman, in *Handbook of Magnetism and Advanced Magnetic Materials*, edited by H. Kronmuller and S. Parkin, Vol. 1: Fundamentals and Theory (John Wiley and Sons, 2007), pp. 95–148.
[22] P.-Y. Chang, O. Erten, and P. Coleman, Nat. Phys. **13**, 794 (2017).
[23] M. Dzero, K. Sun, V. Galitski, and P. Coleman, Phys. Rev. Lett. **104**, 106408 (2010).
[24] J. H. Pixley, S. B. Lee, B. Brandom, and S. A. Parameswaran, Phys. Rev. B **96**, 081105(R) (2017).
[25] M. Z. Hasan and C. L. Kane, Rev. Mod. Phys. **82**, 3045 (2010).
[26] X.-L. Qi and S.-C. Zhang, Rev. Mod. Phys. **83**, 1057 (2011).
[27] B. A. Bernevig and T. L. Hughes, *Topological Insulators and Topological Superconductors* (Princeton University Press, Princeton, NJ, 2013).
[28] B. S. Shastry and B. Sutherland, Physica B+C **108**, 1069 (1981).
[29] C. L. Kane and E. J. Mele, Phys. Rev. Lett. **95**, 146802 (2005).
[30] L. Fu and C. L. Kane, Phys. Rev. B **76**, 045302 (2007).
[31] T. L. Hughes, E. Prodan, and B. A. Bernevig, Phys. Rev. B **83**, 245132 (2011).
[32] B. Sriram Shastry and B. Kumar, Prog. Theor. Phys. Suppl. **145**, 1 (2002).
[33] T. Kariyado and Y. Hatsugai, Phys. Rev. B **88**, 245126 (2013).
[34] C.-K. Chiu, J. C. Y. Teo, A. P. Schnyder, and S. Ryu, Rev. Mod. Phys. **88**, 035005 (2016).
[35] F. D. M. Haldane, Phys. Rev. Lett. **61**, 2015 (1988).
[36] C. L. Kane and E. J. Mele, Phys. Rev. Lett. **95**, 226801 (2005).
[37] T. Kariyado and Y. Hatsugai, in *Proceedings of the 12th Asia Pacific Physics Conference (APPC12)* [JPS Conf. Proc. **1**, 012001 (2014)].
[38] B. I. Halperin, Phys. Rev. B **25**, 2185 (1982).
[39] C. Xu and J. E. Moore, Phys. Rev. B **73**, 045322 (2006).
[40] L. Sheng, D. N. Sheng, C. S. Ting, and F. D. M. Haldane, Phys. Rev. Lett. **95**, 136602 (2005).
[41] D. N. Sheng, Z. Y. Weng, L. Sheng, and F. D. M. Haldane, Phys. Rev. Lett. **97**, 036808 (2006).